



An Approximate Analytical Solution of Non-Linear Fractional-Order Constrained Optimization Problem Using Optimal Homotopy Analysis Method

Oluwaseun Olumide Okundalaye ¹, Wan Ainun Mior Othman ^{1*}

¹ Institute of Mathematical Sciences, Faculty of Science, University of Malaya, MALAYSIA.

*Corresponding Author (Email: wainainun@um.edu.my)

Paper ID: 12A1D

Volume 12 Issue 1

Received 04 August 2020

Received in revised form 08 October 2020

Accepted 22 October 2020

Available online 29 October 2020

Keywords:

Penalty Function;
Fractional Differential Equations; Constrained Optimization Problem; Convergence-Control Parameters; Homotopy Analysis Method.

Abstract

We present an optimal homotopy analysis method (OHAM) to find an accurate approximate analytic solution (AAS) for non-linear fractional-order constrained optimization problem (FOCOP). The previous analytical approximate method (AAM) of solving FOCOP possesses no norms for the convergence of the infinite series solution. OHAM provides an independent way of choosing proper values of the control-convergence parameter (CCP), auxiliary linear operator, and enables us to control and govern the convergence area of the series solution produced by a squared residual error optimization technique. Numerical comparisons of OHAM with Runge-Kutta fourth-order (RK4) method for accuracy. Some examples from the CUTER library were used to indicate the correctness and relevance of the suggested techniques.

Disciplinary: Mathematics.

©2020 INT TRANS J ENG MANAG SCI TECH.

Cite This Article:

Saad, A. M., Mohamad, M. B., and Tsong, C. K. (2021). Hedonic Price Model of Secondhand Condominium Units in Bangkok. *International Transaction Journal of Engineering, Management, & Applied Sciences & Technologies*, 12(1), 12A1D, 1-14. <http://TUENGR.COM/V12/12A1D.pdf> DOI: 10.14456/ITJEMAST.2021.4

1 Introduction

In optimization, different methods had been considered by several authors for solving constrained non-linear programming optimization problems in a class of integer-order systems of ordinary differential equations (ODEs). The gradient-based steepest descent approach is a solution method. The procedure converts a non-linear problem of optimization to systems of non-linear ODE dynamic with optimality requirements to get optimal solutions (Franceschi et. Al., 2017).

The computation of fractional-order began receiving much importance in the area of applied science some years back. Some authors in optimization focused on improving AAM for solving

various forms of arbitrary-order gradient-based dynamic systems from optimization problem: Such as a fractional dynamics trajectory approach (Evirgen and Özdemir, 2012), fractional steepest descent approach (Pu et al., 2013), an arbitrary gradient-based system using VIM (Evirgen, 2016), and a conformable fractional gradient-based system (Evirgen, 2017).

One-step OHAM was developed by Niu and Wang (2010) for non-linear differential equations (NLDEs). Liao (2010) proposed OHAM strong NLDEs to obtain an optimal convergence-control parameter by using optimization a method called squared residual error, which was integrated into the whole region of the governing equation for accurate optimal convergence-control parameters. OHAM approach has still not been implemented in solving non-linear FOCOP, which motivates this study.

2 Preliminaries

We begin by defining some particular functions and properties of fractional calculus (Abdeljawad, 2015).

Definition 1

Let $g: [0, \infty) \rightarrow \mathfrak{R}$ be a given function. The β^{th} order conformable fractional derivative operator of g given by

$$T^\beta(g)(x) = \lim_{\epsilon \rightarrow 0} \frac{g(x+\epsilon x^{1-\beta})-g(x)}{\epsilon} \quad (1),$$

$$\forall x > 0 \text{ and } \beta \in (0, 1].$$

Theorem 1

The function $\frac{d^\beta g}{dx^\beta} = x^{1-\beta} \frac{dg}{dx}$, if g is differentiable, $0 < \beta \leq 1$, and (f, g) be β -differentiable at a point $x > 0$.

Definition 2

Given that the integral is the regular Riemann improper, then we have

$$I_a^\beta(g)(x) = I_a^1(x^{\beta-1}g) = \int_a^x \frac{g(t)}{t^{1-\beta}} dt, \text{ where } t, \text{ and } \beta \in (0, 1].$$

Theorem 2

$T^\beta I_a^\beta(g)(x) = g(x)$, given that g is a continuous function in the domain of I^β and $x \geq a$.

Theorem 3

Let $g: (a, b) \rightarrow \mathfrak{R}$ be differentiable and $0 < \beta \leq 1$. And so for all $x > a$, we have

$$I_a^\beta T^\beta(f)(x) = g(x) - g(a).$$

Taking non-linear programming, constrained optimization problem (NLPCOP) of the figure

$$\min_{x \in \mathfrak{R}^n} g(x) \text{ subject to } \psi_k(x) \leq 0 \text{ and } h_k(x) = 0 \quad \forall k \in \mathfrak{R}. \quad (2),$$

where $g: \mathfrak{R}^n \rightarrow \mathfrak{R}$, $\psi_k: \mathfrak{R}^n \rightarrow \mathfrak{R}$, and $h_k: \mathfrak{R}^n \rightarrow \mathfrak{R}$, $k \in \mathfrak{R}$, are C^2 functions. Let $X_0 = \{x \in \mathfrak{R}^n | h_k = 0, \psi_k \leq 0, k \in \mathfrak{R}\}$ be the feasible set of Equation (2), and X_0 is a set of functions. An efficient penalty function of Equation (2) is given as

$$P_{penalty}(h_k(x)) = \varrho \frac{1}{\sigma} \sum_{k=1}^p (h_k(x))^\sigma, \quad (3),$$

$$P_{penalty}(\psi_k(x)) = \varrho \sum_{k=1}^p (\max\{0, \psi_k(x)\})^\sigma. \quad (4),$$

where $\sigma = 2$. It can be understood from previous research that the solution to Equation (2) is of the unconstrained form given as

$$\min G(x, \varrho) = g(x) + \varrho \left(\frac{1}{\sigma} \sum_{k=1}^p (h_k(x))^\sigma + \sum_{k=1}^p (\max\{0, \psi_k(x)\})^\sigma \right) \quad (5),$$

subject to $x \in \mathfrak{R}^n$

where $\varrho > 0$ is an auxiliary penalty variable (Nguyen et al., 2019).

Using Equation (1) and Equation (2) for problem Equation (5) with $\sigma = 2$, the conformable operator gradient-based dynamic model is formulated as

$$T^\beta x_t = -\nabla_x G(x, \varrho). \quad (6),$$

with the given initial conditions

$$x_k(0) = x_{k0} \quad k = 1 \dots n. \quad (7),$$

where $\nabla_x G(x, \varrho)$ is the gradient vector and $x \in \mathfrak{R}$. This form of optimization problem solution was first introduced in Evirgen and Özdemir (2011).

Note that a point x_e it is an equilibrium point of Equation (6) if it correspondent to the right-hand side of Equation (6). We reformulate the arbitrary-order dynamic system Equation (6) as

$$T^\beta x_k(t) = g_k(t, \varrho, x_1, x_2 \dots x_n), \quad k = 1, 2 \dots n \quad (8).$$

3 Methodology

We solve Equation (8) by constructing homotopy of the form

$$T^\beta x_k(t) = p g_k(t, \varrho, x_1, x_2 \dots x_n) \quad (9),$$

where $k = 1, 2 \dots n$, and $p \in [0, 1]$. If $p = 0$, Equation (9) becomes

$$T^\beta x_k(t) = 0. \quad (10)$$

and when $p = 1$, the homotopy Equation (9)

$$T^\beta x_k(t) = g_k(t, \varrho, x_1, x_2 \dots x_n) \quad t \geq 0, \quad 0 < \beta \leq 1. \quad (11)$$

with given initial conditions

$$x_k(0) = a_k, \quad k = 1, 2 \dots n \quad (12).$$

From (Liao, 2010), we formulate the zeroth-order deformation equations

$$(1 - q)\ell_k[T^\beta \phi_k(t, q) - x_{k0}(t)] = q\hbar_k[T^\beta \phi_k(t, q) - g_k(t, \varrho, \phi_1(t, q), \phi_2(t, q) \dots \phi_n(t, q))] \quad (13),$$

$$k = 1, 2 \dots n$$

where $q \in [0, 1]$ is an enclosed parameter, ℓ_k Are auxiliary linear operators satisfying $\ell_k(0) = 0$, $x_{k0}(t)$ are guessing approximation $x_k(t)$, $\hbar_k \neq 0$ are converging-control parameters, and $\phi_k(t, q)$ are unknown functions, when $q = 0$, and $q = 1$ we have

$$\phi_k(t, 0) = x_{k0}(t), \quad \phi_k(t, 1) = x_k(t) \quad k = 1, 2, 3 \dots n \quad (14).$$

Thus, as q increasing from 0 to 1, the solution $\phi_k(t, q)$ ranges from the initial guess $x_{k0}(t)$ to the solutions $x_k(t)$. Expand $\phi_k(t, q)$ in a Taylor series for q , we have

$$\phi_k(t, q) = x_{k0}(t) + \sum_{m=1}^{\infty} x_{km}(t)q^m \quad (15),$$

where

$$x_{km}(t) = \frac{1}{m!} \frac{\partial^m \phi_k(t, q)}{\partial q^m} \Big|_{q=0}, \quad (16).$$

If the auxiliary linear operators ℓ_k , Convergence-control parameters \hbar_k , And the guess approximation $x_{k0}(t)$, are correctly selected, then the series Equation (15) converges at $q = 1$, one has

$$x_k(t) = x_{k0}(t) + \sum_{m=1}^{\infty} x_{km}(t) \quad k = 1, 2, 3 \dots n \quad (17).$$

As proposed by Odibat (2019), differentiating Equation (13) m -times with for the enclosed parameter q , and equating $q = 0$, and finally subdivide them by $m!$ we have the m th-order equation as

$$\ell_k[x_{km}(t) - \chi_m x_{k(m-1)}(t)] = \hbar_k \mathfrak{R}_{km}(\tilde{x}_{k(m-1)}(t)) \quad (18),$$

where

$$\mathfrak{R}_{km}(\tilde{x}_{k(m-1)}(t)) = \frac{1}{(m-1)!} \frac{\partial^{m-1}}{\partial q^{m-1}} [T^\beta \phi_k(t, q) - g_k(t, \varrho, \phi_1(t, q), \phi_2(t, q), \dots, \phi_n(t, q))] \quad (19),$$

$$k = 1, 2, \dots, n$$

with

$$\chi_m = \begin{cases} 0 & m \leq 1 \\ 1 & m > 1. \end{cases}$$

Multiply both sides of Equation (18) by ℓ_k^{-1} and choose

$$\ell_k^{-1} = I^\beta \quad k = 1, 2, \dots, n.$$

We have

$$x_{km}(t) = \chi_m x_{k(m-1)}(t) + \hbar_k I^\beta [\mathfrak{R}_{km}(\tilde{x}_{k(m-1)}(t))] \quad (20).$$

The m th-order Equation (18), which is linear, can be determined by any symbolic computation Maple software. From Equation (20), we get a power series solution

$$x_k(t) = \sum_{m=0}^{\infty} x_{km}(t) \quad 1 \leq k \leq n \quad (21).$$

When $m \rightarrow \infty$ in Equation (21), we can get an accurate AAS of Eq. (3.4). The traditional approach to get interval values for convergence-control parameters \hbar_k is to plot the \hbar_k -Curve by drawing a curve of a certain proportion versus \hbar_k . Afterward, it was found that the traditional approach could not yield optimal values as declared by (Liao, 2010), which made (Odibat, 2020)

suggesting an optimization method for the optimal value of CCP by using squared residual error. Power series solution Equation (21) relies upon the convergence-control parameter vector.

The squared residual error in the m th-order of AAS is given as

$$\Delta(\hbar_1, \hbar_2) = \sum_{j=1}^2 \int_{\Omega} (N_j[\sum_{k=0}^m x_1, \sum_{k=0}^m x_2])^2 d\Omega. \quad (22).$$

denotes the square residual error of the governing equation Equation (2) at the m th-order of approximation, where $m=1, 2$, and so on. At the first-order of an estimate, the squared residual error Δ_k are depending on \hbar_k and the optimal values for \hbar_k are obtained by solving non-linear algebraic equations

$$\frac{\partial \Delta(\hbar_k)}{\partial \hbar_k} = 0 \quad k = 1, 2, \dots, n. \quad (23).$$

3.1 The Convergence Analysis

Theorem 1. As long as the series $x_k(t) = x_{k0}(t) + \sum_{m=1}^{\infty} x_{km}(t)$ for $k = 1, 2, 3, \dots, n$ converges where $x_{km}(t)$ is governed by Equation (18) under the definition Equation (19), it must be the result of Equation (11).

Proof: If we consider $\sum_{m=1}^{\infty} x_{km}(t)$ for $k = 1, 2, 3, \dots, n$ converges to $x_k(t)$ then

$$\lim_{m \rightarrow \infty} x_{km}(t) = 0 \quad \forall \quad k = 1, 2, \dots, n \quad (24).$$

We can write

$$\sum_{m=1}^{\infty} \hbar_k \mathfrak{R}_{km}(\tilde{x}_{k(m-1)}(t)) = \sum_{m=1}^{\infty} \ell_k [x_{km}(t) - \chi_m x_{m-1}(t)], \quad (25)$$

$$= \lim_{n \rightarrow \infty} \sum_{m=1}^n \ell_k [x_{km}(t) - \chi_m x_{m-1}(t)], \quad (26)$$

$$= \ell_k x_{11}(t) + (\ell_k x_{22}(t) - \ell_k x_{21}(t)) + (\ell_k x_{nn}(t) - \ell_k x_{n(n-1)}(t)), \quad (27)$$

$$= \ell_k \left[\lim_{n \rightarrow \infty} \sum_{m=1}^n x_{nn}(t) \right], \quad (28)$$

$$= \ell_k \left[\lim_{n \rightarrow \infty} x_{nn}(t) \right] = 0 \quad \forall \quad k = 1, 2, \dots, n. \quad (29).$$

Since $\hbar_k \neq 0$,

$$\mathfrak{R}_{km}(\tilde{x}_{k(m-1)}(t)) = 0. \quad (30)$$

Hence, using the above

$$\sum_{m=1}^{\infty} \mathfrak{R}_{km}(\tilde{x}_{k(m-1)}(t)) = \sum_{m=1}^{\infty} [T^\beta x_{k(m-1)} - g_k(t, \varrho, x_{1(m-1)}, x_{2(m-1)} \dots \dots x_{n(m-1)})]$$

$$= \sum_{m=1}^{\infty} T^\beta x_{k(m-1)} - \sum_{m=1}^{\infty} g_k(t, \varrho, x_{k(m-1)}) \quad (32)$$

$$= T^\beta x_k t - g_k(t, \varrho, x_k(t)) \quad (33).$$

From Equations (30) and (33), we have

$$T^\beta x_k(t) = g_k(t, \varrho, x_k(t)) \quad \forall \quad k = 1, 2, \dots, n \quad (36)$$

4 Numerical Examples and Results

Example 1: We consider test problem from (Schittkowski, 2012) [No 216]

$$\text{minimize } g(x) = 100(x_1^2 - x_2)^2 + (x_1 - 1)^2 \quad (37),$$

$$\text{subject to } h(x) = x_1(x_1 - 4) - 2x_2 + 12 = 0 \quad (38),$$

$$x_0 = (0, 0) \quad (39),$$

whose analytical solution is unknown, but the intended optimal solution is $x_1^* = 1.9993, x_2^* = 3.9998$. From Equation (5), we have

$$G(x, \varrho) = 100(x_1^2 - x_2)^2 + (x_1 - 1)^2 + \frac{1}{2}\varrho(x_1(x_1 - 4) - 2x_2 + 12)^2 \quad (40).$$

Similarly from Equation (6), for $\varrho = 200$ gives

$$T^\beta x_1(t) = -400(x_1^2 - x_2)x_1 - 2(x_1 - 1) - \varrho(2x_1 - 4)(x_1^2 - 4x_1 - 2x_2 + 12) \quad (41),$$

$$T^\beta x_2(t) = 200(x_1^2 - x_2) + 2\varrho(x_1^2 - 4x_1 - 2x_2 + 12) \quad 0 < \beta \leq 1, \quad (42),$$

$$x_1(0) = 0, \quad x_2(0) = 0 \quad (43).$$

Chosen a linear operator of the form

$$\ell_k^{-1} = I^\beta, \quad k = 1, 2, \dots, n,$$

According to the formula Equation (19), we have

$$\begin{aligned} \mathfrak{R}_{1m}(\tilde{x}_{1(m-1)}(t), \tilde{x}_{2(m-1)}(t)) = & T^\beta x_{1[m-1]} - 2000 \sum_{k=0}^{m-1} x_{1[m-1-k]} \sum_{j=0}^n x_{1[k-j]} x_{1[j]} - \\ & 9600 \sum_{k=0}^{m-1} x_{1[m-1-k]} x_{1[k]} + 32002 x_{1[m-1]} + 3600 x_{1[m-1]} x_{2[m-1]} + 6400 x_{2[m-1]} - \\ & 38402(1 - \chi_m), \end{aligned} \quad (44),$$

$$\begin{aligned} \mathfrak{R}_{2m}(\tilde{x}_{1(m-1)}(t), \tilde{x}_{2(m-1)}(t)) = & T^\beta x_{2[m-1]} - 1800 \sum_{k=0}^{m-1} x_{2[m-1-k]} x_{2[k]} - 3200 x_{1[m-1]} - \\ & 1800 x_{2[m-1]} + 9600(1 - \chi_m), \end{aligned} \quad (45)$$

and the m th -order for $m \geq 1$ become

$$x_{1m}(t) = \chi_m x_{1[m-1]}(t) + \hbar_1 I^\beta [\mathfrak{R}_{1m}(\overline{\tilde{x}}_{1[m-1]}(t))] \quad (46),$$

$$x_{2m}(t) = \chi_m x_{2[m-1]}(t) + \hbar_2 I^\beta [\mathfrak{R}_{2m}(\overline{\tilde{x}}_{2[m-1]}(t))] \quad (47).$$

From Equation (46) and Equation (47) above, we generate symbolic series solutions for Equation (41) and Equation (42) as:

$$x_1(1) = 38402 \hbar_1 t, \quad (48)$$

$$x_2(1) = 9600 \hbar_2 t, \quad (49)$$

$$x_1(2) = 4.423910400 \times 10^1 \hbar_2 t^3 \hbar_1^2 + \hbar_1 (-6.144704020 \times 10^8 \hbar_1 + (3.0720000 \times 10^7 \hbar_2) t^2 + 38402 \hbar_1 t + \dots \quad (50)$$

$$x_2(2) = 9600 \hbar_2 t + 8727.272727 \hbar_2^2 t^{\frac{11}{10}} - 9.6005000 \times 10^7 \hbar_2 t^2 \hbar_1 \quad (51)$$

From Equation (22), the "optimal values" of (\hbar_1, \hbar_2) is estimated by

$$\frac{\partial \Delta(\hbar_1, \hbar_2)}{\partial \hbar_1} = 0, \quad \frac{\partial \Delta(\hbar_1, \hbar_2)}{\partial \hbar_2} = 0 \quad (52).$$

It is found that

$$\Delta_1(1) = 1.636236158 \times 10^{16} - 7.612634534 \times 10^{20} \hbar_1 - 2.171187483 \times 10^{25} \hbar_1^2 - 2.004277445 \times 10^{28} \hbar_1^3 - 8.154151650 \times 10^{19} \hbar_2 + 1.409110792 \times 10^{24} \hbar_1 \hbar_2 \quad (53)$$

$$\Delta_2(1) = 1.414477488 \times 10^{15} + 2.038537912 \times 10^{19} \hbar_2 \quad (54)$$

Our calculations indicated that, $\Delta_1(3)$ and $\Delta_2(3)$ has its minimum values at

$$\Delta_1(3) = -2.149 \times 10^{17} \text{ and } \Delta_2(3) = -2.678 \times 10^{11}.$$

and we have $\hbar_1 = 0.1041094886$, $\hbar_2 = -0.6938686201$ that gives an optimal solution to the problem

Example 2: We consider test problem from (Schittkowski, 2012) [No 1]

$$\text{minimize } g(x) = 100(x_2 - x_1^2)^2 + (1 - x_1)^2 \quad (55)$$

$$\text{subject to } \psi(x) = 1.5 \leq x_2 \quad (56)$$

$$x_0 = (-2, 1) \quad (57)$$

whose analytical solution is unknown, but the intended optimal solution is $x_1^* = 1$, $x_2^* = 1$. From Equation (5), we have

$$G(x, \rho) = 100(x_2 - x_1^2)^2 + (1 - x_1)^2 + \rho(\max\{0, -1.5 - x_2\})^2 \quad (58)$$

Taking the differentiation of Equation (58), we have

$$T^\beta x_1(t) = -400x_1^3 + 400x_1x_2 - 2x_1 + 2, \quad (59)$$

$$T^\beta x_2(t) = 200x_1^2 - 200x_2, \quad (60)$$

$$x_1(0) = 0, \quad x_2(0) = 0. \quad (61)$$

Following the same procedure above, we have

$$x_1(1) = -794 \hbar_1 t, \quad (62)$$

$$x_2(1) = 600 \hbar_2 t, \quad (63)$$

$$x_1(2) = -8.069580800 \times 10^{12} \hbar_1^4 \hbar_2 t^5 + 1.260872000 \times 10^8 \hbar_1^4 t^4 - 1.479028739 \times 10^8 t^{\frac{31}{10}} \hbar_1^4 + \dots \quad (64)$$

$$x_2(2) = (-60000 \hbar_2^2 + 317600 \hbar_1 \hbar_2) t^2 + 545.4545455 \hbar_2^2 t^{\frac{11}{10}} + 600 \hbar_2 t \quad (65)$$

and so on.

Our estimation showed that $\Delta_1(3)$ and $\Delta_2(3)$ has its minimum results at

$$\Delta_1(3) = -0.149 \times 10^{17}, \Delta_2(3) = 0.124 \times 10^{11}.$$

The optimal value of h_1, h_2 Are determine as $h_1 = -0.05346$ and $h_2 = 0.07546$.

Table 1: The relation and absolute error among (OHAM, $\beta = 1$) and (RK4, $\beta = 1$) solutions, of **example 1**.

t_k	OHAM $x_1(t)$	OHAM $x_2(t)$	RK4 $x_1(t)$	RK4 $x_2(t)$	Abs error $x_1(t)$	Abs error $x_2(t)$
0.0000	0.000000	0.000000	0.000000	0.000000	0.000000	0.000000
0.0005	1.970111	3.871642	1.970899	3.871887	0.000788	0.000245
0.0010	1.977113	3.907789	1.978274	3.907993	0.001161	0.000204
0.0015	1.981099	3.922324	1.981384	3.922554	0.000285	0.00023
0.0018	1.982155	3.930478	1.983132	3.930578	0.000977	0.00010
0.0020	1.993105	3.995556	1.994252	3.995654	0.001147	0.000098

Tables 1 and 2 show the analytical approximate and numerical values, for **example 1**, and **example 2** at a different time (t). It can be understood that the analytical approximate and numerical values are in close correspondence with a deficient absolute error, which makes OHAM an excellent method to solve non-linear FOCOP.

Table 2: The relation and absolute error among (OHAM, $\beta = 1$) and (RK4, $\beta = 1$) solutions of **example 2**.

t_k	OHAM $x_1(t)$	OHAM $x_2(t)$	RK4 $x_1(t)$	RK4 $x_2(t)$	Abs error $x_1(t)$	Abs error $x_2(t)$
0.0	0.000000	0.000000	0.000000	0.000000	0.000000	0.000000
2.0	0.156230	0.023457	0.161481	0.023694	0.005251	0.000237
4.0	0.691769	0.578784	0.693706	0.579773	0.001937	0.000989
6.0	0.830467	0.788985	0.830548	0.789065	8.1E-05	8E-05
8.0	0.917518	0.970234	0.927053	0.970426	0.009535	0.000192
10.0	0.997398	0.987894	0.998826	0.993629	0.001428	0.005735

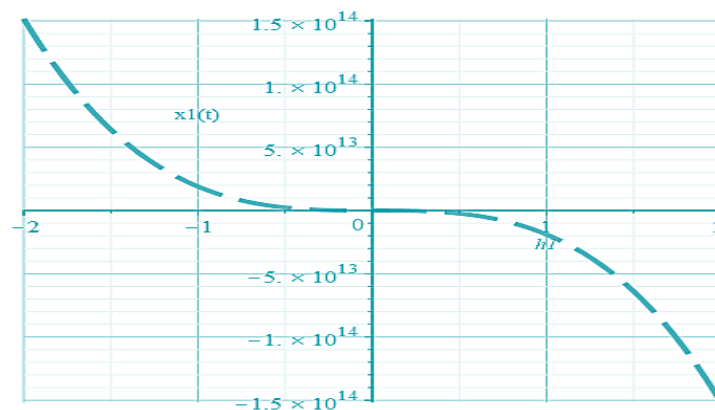


Figure 1. The h1-curve of OHAM for example 1 at (t=0.005) of $x_1(t)$.

The h1-curve in Figure 1 shows the convergence domain of the solution of **example 1**, between an interval of $-0.5 < h_1 < 0.5$ at $x_1(t)$ and provides a clear region of the optimal values for the convergence of the proposed solution method. Figure 2 shows the domains of convergence of the series solution given by h2 at $x_2(t)$ of example 1 and provided a clear region of the optimal values for the convergence of the proposed solution method.

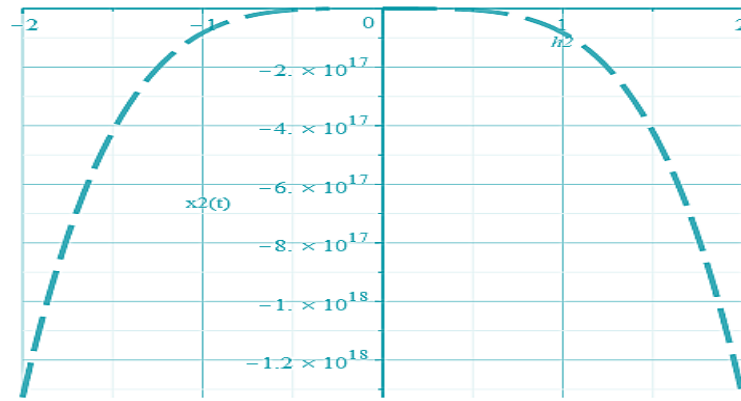


Figure 2: The h2-curve of OHAM for example 1 at (t=0.005) of $x_2(t)$.

Figures 3 and 4 shows mathematical simulations of the proposed method at $x_1(t)$ and $x_2(t)$ of example 1, respectively. The mathematical simulation illustrates OHAM solution as an excellent tool to solve the problem.

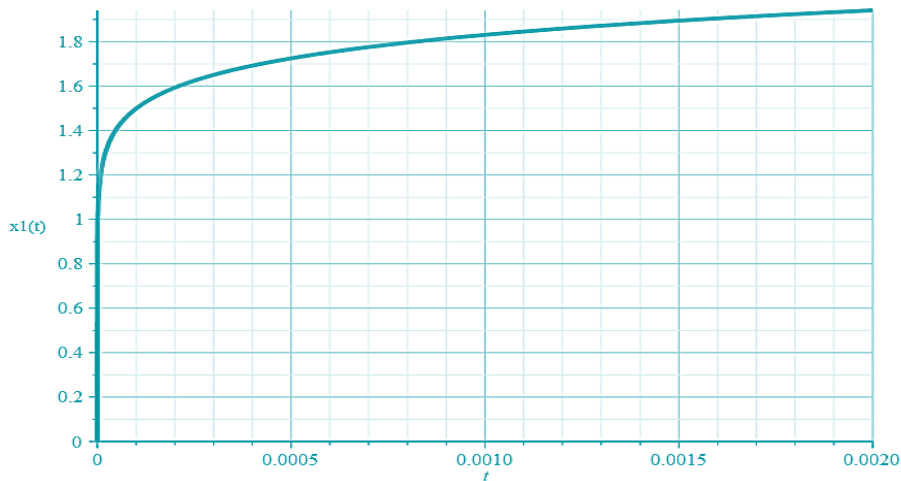


Figure 3. The mathematical simulation of OHAM solution for $\beta=0.9$ of **example 1** at the third-order approximation of $x_1(t)$.

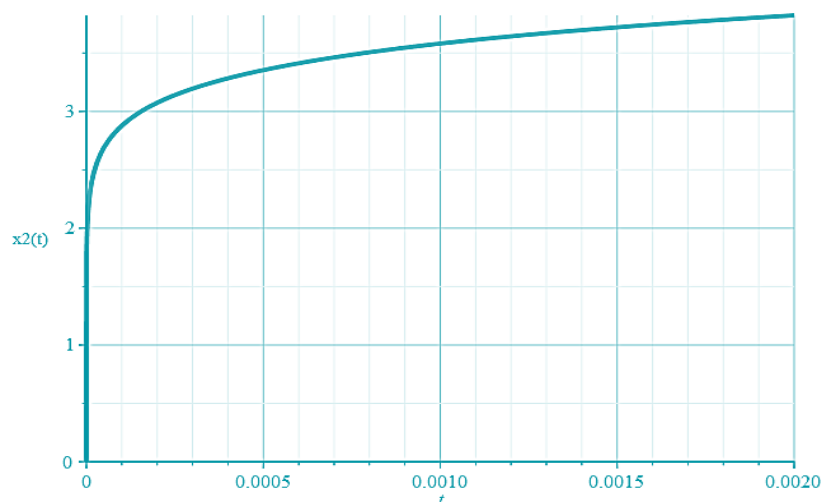


Figure 4. The mathematical simulation of OHAM solution for $\beta=0$. For **example 1** at the third-order approximation of $x_2(t)$.

Figures 5 and 6 shows the comparisons between different values of OHAM and RK4 method for justification at $x_1(t)$ and $x_2(t)$ of example 1. The comparison shows that OHAM would perform fast convergence to the optimal solutions. From Figure 6, the solution from OHAM is very precise with the expected optimal solution as the values of $(\beta=1)$ approaches 1. The h1-curve in Figure 7 shows the domain of convergence of the series solution of example 2, between an interval of $-1 < h_1 < 1$ at $x_1(t)$.

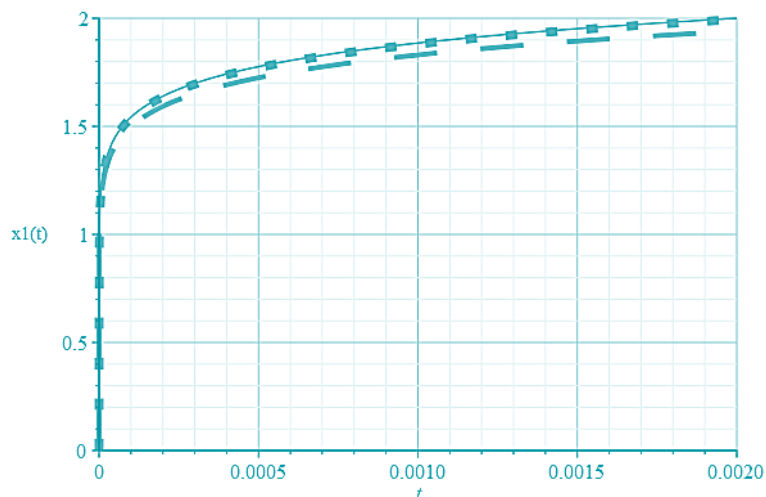


Figure 5. Comparisons between OHAM ($\beta = 0.9$, *space dash*, $\beta = 1$, *dot*) and RK4 ($\beta = 1$, *solid*) at $x_1(t)$ of example 1. It is seen in figure 5 that the solution from OHAM is very precise with the expected optimal solution as the values of $(\beta=1)$ approaches 1.

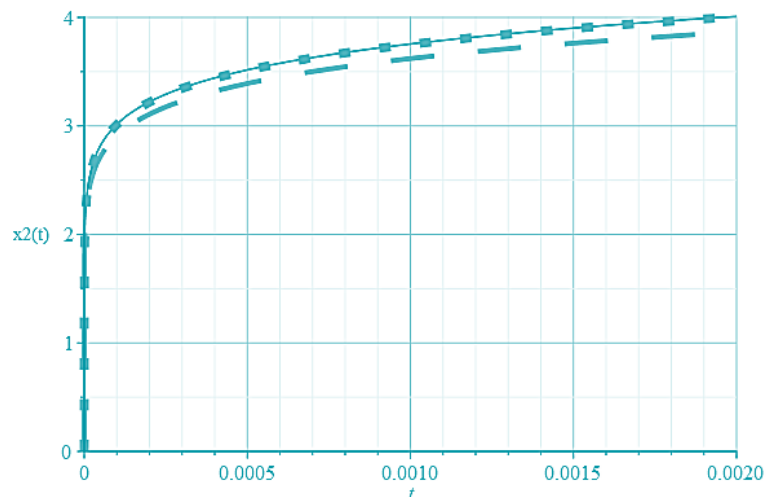


Figure 6. Comparisons between OHAM ($\beta = 0.9$, *space dash*, $\beta = 1$, *dot*) and RK4 ($\beta = 1$, *solid*) at $x_2(t)$ of example 1.

Figure 7 shows the domains of convergence of the series solution given by h_1 at $x_1(t)$ and h_2 at $x_2(t)$ of example 2 and provided a clear region of the optimal values for the convergence of the proposed solution method.

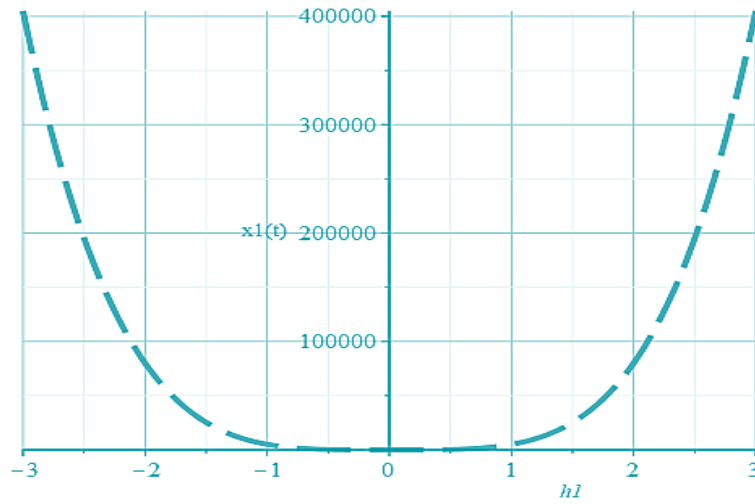


Figure 7. The h_1 -curve of OHAM, for example 2 at $(t=2)$ of $x_1(t)$.

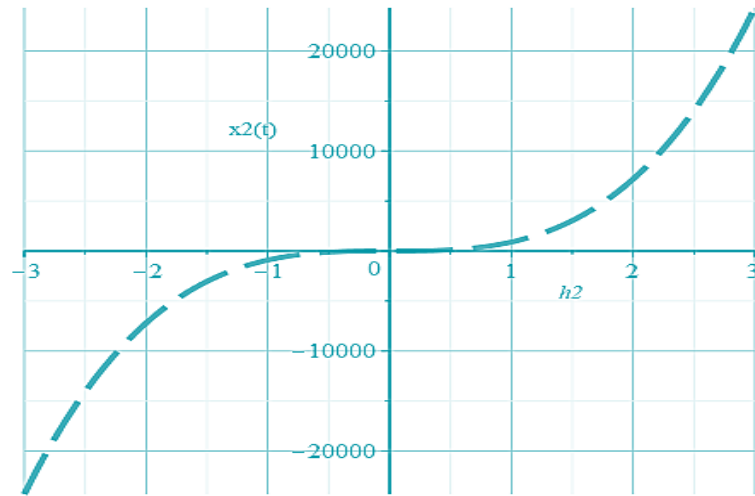


Figure 8. The h_2 -curve of OHAM, for example 2 at $(t=2)$ of $x_2(t)$. The h_2 -curve in figure 8 shows the domain of convergence of the series solution of example 2, between an interval of $-1 < h_2 < 1$ at $x_2(t)$.

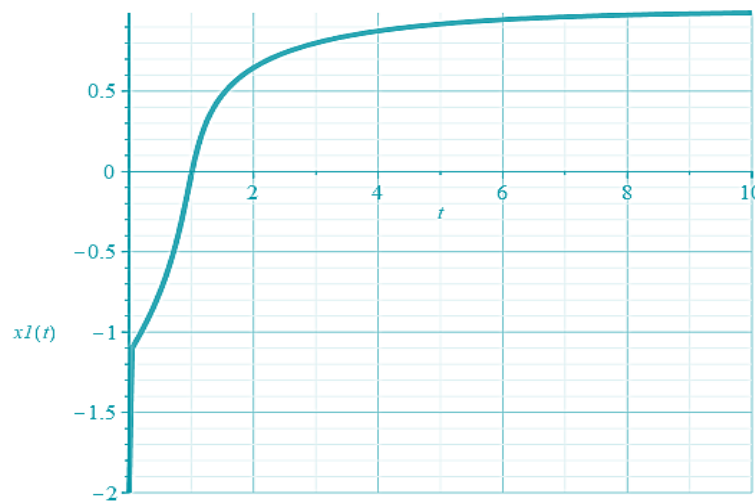


Figure 9. The mathematical simulation of OHAM solution for $\beta=0$. For example 2 at the third-order approximation of $x_1(t)$.

Figures 9 and 10 show mathematical simulations of the proposed method at $x_1(t)$ and $x_2(t)$ of example 2. The mathematical simulation illustrates OHAM solution as an excellent tool to solve the problem.

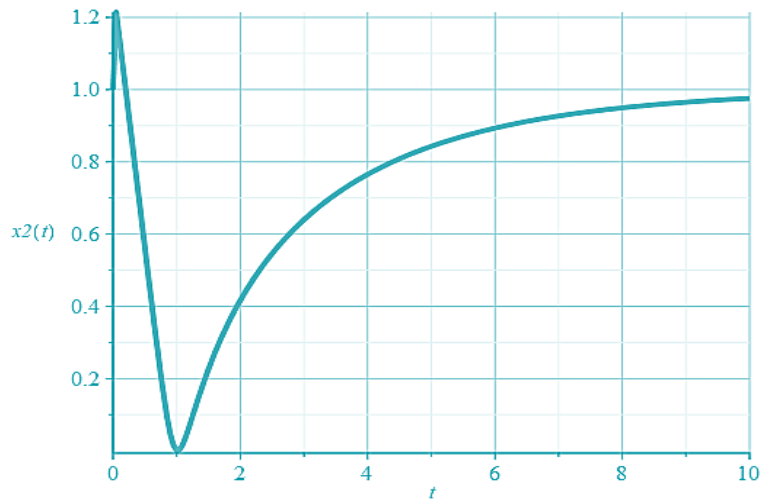


Figure 10. The mathematical simulation of OHAM solution for $\beta=0$. For **example 2** at the third-order approximation of $x_2(t)$.

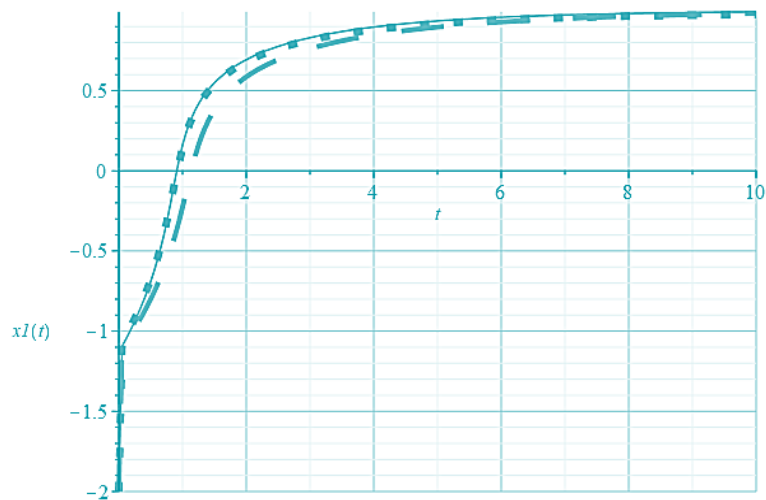


Figure 11. Comparisons between OHAM ($\beta = 0.9$, *space dash*, $\beta = 1$, *dot*) and RK4 ($\beta = 1$, *solid*) at $x_1(t)$ of **example 2**.

It is seen in Figure 11 that the solution from OHAM is very precise with the expected optimal solution as the values of ($\beta=1$) approaches 1. From Figure 12, the solution from OHAM is very precise with the expected optimal solution as the values of ($\beta=1$) approaches 1

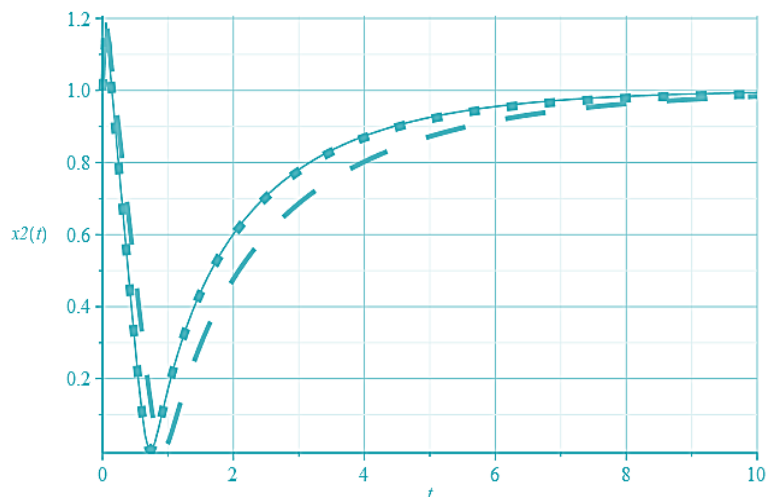


Figure 12. Comparisons between OHAM ($\beta = 0.9$, *space dash*, $\beta = 1$, *dot*) and RK4 ($\beta = 1$, *solid*) at $x_2(t)$ of **example 2**.

5 Discussion

The results are given by (\hbar_1, \hbar_2) Using OHAM shows the strength of the method on the convergence of the series solution through h-curves plots of the systems for $(\beta=0.9, 1)$. We showed that even three-order terms of the analytical approximation of the solutions are enough to get an accurate solution. It is understandably that the exactness can be optimized by computing a few more terms of the approximate analytical solutions.

6 Conclusion

This paper solved non-linear FOCOP by OHAM after the third order of approximation solution was used with fast convergence and accurate solutions. The numerical comparison among the RK4 and OHAM $(\beta=1)$, shows that OHAM would perform fast convergence to the optimal solutions as $(\beta=1)$ tends to 1, the integer-order solution for the system is reclaimed. OHAM is an effective tool for obtaining an AAS for non-linear FOCOP.

7 Availability of Data and Material

Information can be made available by contacting the corresponding author.

8 References

- Abdeljawad T. (2015). On conformable fractional calculus. *Journal of Computational & Applied Mathematics*, 279, 57-66.
- Evirgen F, Özdemir N. (2011). Multistage domain decomposition method for solving NLP problems over a non-linear fractional dynamical system. *Journal of Computational & Nonlinear Dynamics*, 6(2).
- Evirgen F, Özdemir N. (2012). A fractional-order dynamical trajectory approach for optimization problem with HPM. *Fractional Dynamics & Control*, 145-155.
- Evirgen F. (2016). Analyze the optimal solutions of optimization problems by means of fractional gradient based system using vim. *International Journal of Optimization & Control: Theories & Applications*, 6(2), 75-83.
- Evirgen F. (2017). Conformable fractional gradient based dynamic system for constrained optimization problem. *Acta Physica Polonica A*, 132(3), 1066-1069.
- Franceschi L, Donini M, Frasconi P, Pontil M. (2017). Forward and reverse gradient-based hyperparameter optimization. *Proceedings of the 34th International Conference on Machine Learning*, 70, 1165-1173.
- Liao S. (2010) An optimal homotopy-analysis approach for strongly non-linear differential equations. *Communications in Nonlinear Science & Numerical Simulation*, 15(8), 2003-2016.
- Nguyen BT, Bai Y, Yan X, Yang T. (2019). Perturbed smoothing approach to the lower order exact penalty functions for non-linear inequality constrained optimization. *Tamkang Journal of Mathematics*, 50(1), 37-60.
- Niu Z, Wang C. A. (2010). One-step optimal homotopy analysis method for non-linear differential equations. *Communications in Nonlinear Science and Numerical Simulation*, 15(8), 2026-2036.
- Odibat Z. (2019). On the optimal selection of the linear operator and the initial approximation in the application of the homotopy analysis method to non-linear fractional differential equations. *Applied Numerical Mathematics*, 137, 203-212.
- Odibat Z. (2020). An improved optimal homotopy analysis algorithm for non-linear differential equations. *Journal of Mathematical Analysis and Applications*, 124089.

Pu YF, Zhou JL, Zhang Y, Zhang N, Huang G, Siarry P. (2013). Fractional extreme value adaptive training method: fractional steepest descent approach. *IEEE Transactions on Neural Networks & Learning Systems*, 26(4), 653-662.

Schittkowski K. (2012). *More Test Examples for Nonlinear Programming Codes*. Springer-Verlag, Springer Science & Business Media, 282.



Okundalaye Oluwaseun Olumide is a Ph.D. candidate in the Institute of Mathematical Sciences (ISM), University of Malaya (UM), Malaysia. He received a bachelor's degree in Pure Mathematics at Adekunle Ajasin University, Akungba-Akoko, Nigeria, and a master's degree in optimization at the University of Unilorin, Ilorin, Nigeria. His research interest is in fractional-order gradient-based dynamic system, fractional optimal control problem, and modeling. He focuses on an approximate analytical method to solve the optimization problem in a fractional calculus sense.



Dr. Wan Ainun obtained is Head of the Centre of Mathematical and Statistical Analysis, University of Malaya. She got her B.Sc. and MSc from the University of Charlotte, North Carolina, and North Carolina State University. She got her Ph.D. in the area of Computer-Aided Geometric Design. Her main research interests are in Cryptography, Geometric Modelling, and Differential Equations.
